Neutron Diffraction Study of Liquid *N*-Methylformamide Using EPSR Simulation

João M. M. Cordeiro*,† and Alan K. Soper

ISIS Facility, STFC Rutherford Appleton Laboratory, Harwell Science and Innovation Campus, Didcot, Oxon, OX11 0QX, United Kingdon

Received: March 6, 2009

The structure of *N*-methylformamide (NMF) in liquid state has been investigated using a combination of neutron diffraction measurements augmented with isotopic substitution and empirical potential structure refinement computer simulations. The reference potential used was optimized previously and consisted of Coulomb and 6-12 Lennard-Jones interactions for the atoms. The results show that the three-dimensional model of the liquid structure constructed at the correct atomic number density is consistent with the diffraction experimental data. The liquid structure is orientated by the hydrogen bonds among the molecules. Each NMF molecule is, on average, hydrogen bonded to two others. The findings indicate that dimers and "linear" trimers are very stable species in the liquid bulk. Because of that, the liquid is strongly structured into a chain-like structure. Neighboring chains are stabilized with respect to each other by weak O···H(C) hydrogen bonds. The results are consistent with the known physicochemical properties of the liquid.

I. Introduction

Methods of molecular simulations are powerful tools to investigate molecular interactions in liquid systems as can be noticed from applications of some of those methodologies reported in the past few years.[1−3] In the case of biological molecules, as for instance proteins, however, it is difficult to start by looking at the actual protein molecules due to the great complexity required for the simulation of such a system. Because of this, computationally more suitable smaller systems are commonly used as models to investigate the behavior of a particular feature of an interested system, and the acquired knowledge is then extended to the actual system.

N-Methylformamide (NMF) is one of the simplest molecules that includes a peptide bond in its structure. Because of that, it is widely used in computer simulations to test ideas for peptide interatomic potential functions. These molecules act as proton donor and acceptor via their C═O and N═H groups and consequently form C═O···H═N hydrogen bonds (H-bonds) to each other, the same type of H-bond that is known to play an important role in the stabilization of the ordered intramolecular structure of peptides and proteins in aqueous solution.[4] Moreover, these molecules can also form the so-called C═H···O═C weak H-bonds, which are of great importance in the stabilization of many systems, as has been extensively reported.[5] Some of the most important properties of NMF that make it a popular organic solvent are its very high dielectric constant (ε = 182 at 25 °C),[6] dipole moment μ = 3.86 D[7] or 3.78 D,[8] boiling point 199.5 °C, and heat of vaporization of 13.77 kcal/mol.[9] Such large values for these properties for a molecular liquid have been attributed to the H-bonded network throughout the liquid. The structure of the NMF has been extensively studied experimentally[10−17] as well as theoretically.[11,15−25] Liquid NMF consists of the cis and trans conformers shown in Figure 1 with the OC−NH group adopting the essentially planar peptide bond configuration.[8,11,26]

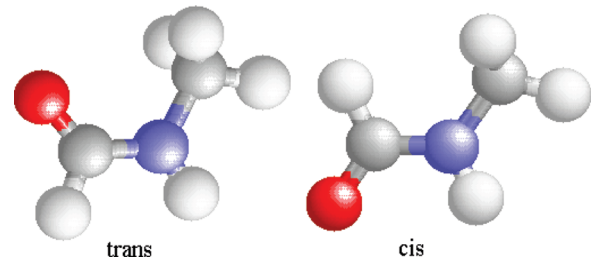

Figure 1. Cis and trans conformers of NMF.

At normal conditions, the population of the trans conformer has been found to be about 94% of the total number of molecules[3,8] which, at first sight, could be seen as a surprise, taking into account steric hindrance (the oxygen and the methyl group are on the same side of the molecule, whereas the hydrogen bonded to nitrogen, much smaller than methyl, stays on the opposite side). Fantoni and Caminati found, at the HF/6-31G** level on Gaussian92, the trans conformer 4.2−5 kJ.mol^{-1} is more stable than the cis form.[8] Hammami et al. used DFT calculations with a standard TZV basis set and polarization exponents[15] and found the trans conformer 6.8 kJ.mol^{-1} to be more stable than the cis conformer, and Cordeiro et al.[27] found the trans conformer 7.87 kJ.mol^{-1} to be more stable than the cis one using DFT calculations with B3LYP functional and MP2 calculations with a 6-311++G** basis set. In these calculations the absolute energy for each conformer depends on the calculation technique used but the difference between the cis and trans energies does not.[27] Ohtaki et al.[11] found with X-ray diffractometry that liquid NMF is mainly constituted of very flexible molecular chains of trans molecules bonded by hydrogen bonds, which has been supported by theoretical results.[20,21] Hammami et al. have concluded, using X-ray and neutron scattering,[15,16] that each trans conformer in the liquid establishes on average two hydrogen bonds with neighboring ones, conferring to the liquid a molecular association that resembles the structure in the crystal NMF. The authors also report, on the basis of the DFT calculations and experimental X-ray scattering, that the local arrangement in the liquid NMF is better described by a

* Corresponding author. E-mail: cordeiro@dfq.feis.unesp.br. Phone: +55 18 3743 1064. Fax: +55 18 3742 4868.
† Universidade Estadual Paulista, Departamento de Física e Química, Av. Brasil, 56, 15385-000, Ilha Solteira, SP, Brazil.

10.1021/jp902053y CCC: $40.75
Published on Web 04/20/2009

ring cis trimer.[15] This seems to be a surprise because the cis monomers exist in the liquid only in the ratio of 5% of the total molecules. Most probably, the cis molecules would have difficulty meeting each other in the liquid bulk to form such trimers. So, the number of these trimers in the liquid, if they exist at all, should be at a very small percentage. Schoester et al. obtained by MD simulations that liquid NMF is composed of a mixture of linear and cyclic species.[17] As discussed previously, NMF−NMF cyclic dimers are more stable than linear dimers.[25] However, the stability of the linear chain increases with the number of monomers in the chain and because of that linear chains prevail over the formation of cyclic dimers on the liquid.[25] The percentage of cyclic dimers in the bulk therefore must be very low.

Despite all those studies, or perhaps because of some of them, there are gaps to be filled to fully understand the behavior of the liquid NMF. Particularly, the presence of H-bonds introduces specific interactions, as for example, a shorter range arrangement among the molecules and a slowing down of the molecular motions,[28] which merits broader investigation. From the point of view of our interest, it is important to achieve a good comprehension of the liquid NMF structure to support our further investigation on the peptide behavior.

Over the past decade, significant advances have been made in the methods of neutron diffraction with isotopic substitution[29] and in the development of reverse Monte Carlo methodology that permits us to convert the resulting experimental data to three-dimensional structural models.[30] The use of hydrogen−deuterium isotopic substitution to enhance the contrast in the experimental scattering patterns confers enhanced reliability on the intermolecular structural information that can be extracted from the resulting model.[29] On the other hand, using the empirical potential structure refinement[31,32] (EPSR) to build a structure of the liquid that is consistent with the measured total structure factors is a way of achieve details on the liquid structure, perhaps not feasible with other methodology, that can be extremely useful in improving the understanding on the liquid behavior. NMF has never been explored with such a methodology before. However, as has been given attention above, the distinctive properties of NMF, its importance as solvent, and the unclear points on its structure justify a new study on it. In this work we present results of a neutron diffraction study using hydrogen−deuterium isotopic substitution and EPSR simulations of the structure of liquid NMF at room temperature.

II. Theoretical Basis

Following corrections, the function extracted from a neutron diffraction experiment is the total structure factor $F(Q)$, which can be written as[33]

$$F(Q) = \sum_{\alpha \le \beta} (2 - \delta_{\alpha\beta}) c_\alpha c_\beta b_\alpha b_\beta (S_{\alpha\beta}(Q) - 1) \qquad (1)$$

and is defined in terms of the magnitude of the scattering vector, Q:

$$Q = \frac{4\pi}{\lambda} \sin\theta \qquad (2)$$

Here λ is the wavelength of the incident neutrons, and 2θ is the scattering angle.

The structure factor contains information relating to the pairwise spatial correlations between atoms of type α and β, reflected in the sum over partial structure factors, $S_{\alpha\beta}(Q)$. These terms are weighted by the respective concentrations, c_α and c_β, and scattering lengths, b_α and b_β, of each atom type. To avoid double counting of the like terms within the summation, $\delta_{\alpha\beta}$ is the Kronecker delta function.

The structure factors, either composite or partial, can be inverted to real space atomic pair distribution function, $g_{\alpha\beta}(r)$, by a Fourier transform weighted by the atomic density, ρ:

$$(S_{\alpha\beta}(Q) - 1) = 4\pi\rho \int_0^\infty r^2 (g_{\alpha\beta}(r) - 1) \frac{\sin Qr}{Qr} \, dr \qquad (3)$$

$g_{\alpha\beta}(r)$ represents the real space correlations between pairs of atoms as a function of their separations, r, and is a primary aim of most structural studies of liquids and disordered materials. Another function that can be extracted from the experimental data and might be useful in the analysis of the material structure from the experimental neutron scattering is the total radial distribution functions, $f(r)$, which are obtained by direct Fourier transform of the inversion of the experimental structure factor data ($F(Q)$).

$$f(r) = \sum_{\alpha \le \beta} (2 - \delta_{\alpha\beta}) c_\alpha c_\beta b_\alpha b_\beta (g_{\alpha\beta}(r) - 1) \qquad (4)$$

To access directly the partial pair distribution function by neutron scattering technique, it is necessary to perform a series of diffraction measurements. In each measurement the contrast of the total structure factor is varied by changing the isotopic composition of the sample. The use of isotopic contrast with neutron diffraction is a powerful probe of local structure, because of the large contrast in neutron scattering length between hydrogen (−3.74 fm) and deuterium (6.77 fm), which greatly assists in delineating the different site−site distribution that are needed to describe the liquid. For systems with more than two atom types, it is generally not possible, or practical, to perform enough isotope variation experiments to extract all the partial structure factors required to completely characterizing the system. The experimental data are thus, more often than not, incomplete with regard to a total solution. Fortunately, modern computational techniques allow us to address successfully this incompleteness problem. What is required is a three-dimensional model of the structure of the disordered system that is consistent with the available experimental data. Classical computational techniques such as Monte Carlo simulation have evolved to the point where obtaining this is straightforward. The underlying premise is that the more experimental data that are used to constrain the model, the more reliable are the final results. Once such a molecular model is available, we can access any site−site partial distribution function of interest as well as evaluate the most likely molecular orientational correlations functions.[34−38]

III. Experimental Methods

The neutron scattering data were collected using the small angle neutron diffractometer for amorphous and liquid sample (SANDALS) at the ISIS pulsed neutron source at the Rutherford Appleton Laboratory, Oxfordshire, U.K. This instrument is optimized for the study of light element-containing liquids and glasses and in particular for hydrogen/deuterium isotopic substitution. The instrument concentrates its neutron detectors at scattering angles (2θ) below 40°, which helps to reduce the effects of nuclear recoil when neutrons are scattered from materials containing hydrogen. To facilitate the direct extraction of intermolecular structural correlations between NMF molecules, three samples were measured: (1) C_2H_5ON, (2) C_2D_5ON, and (3) a 50% mixture of C_2H_5ON and C_2D_5ON. Each sample was contained in a flat plate of internal dimensions 1 mm × 35 mm × 35 mm constructed from a $Ti_{0.68}Zr_{0.32}$ alloy with a wall thickness of 1.1 mm for each surface bounding the inner volume.

TABLE 1: Lennard-Jones, Charge and Atomic Mass Parameters of NMF[25] Used for Reference Potentials within the EPSR

atom type	ε (kJ/mol)	σ (Å)	M (amu)	q (e)
C	0.4389	3.75	12	0.34
O	0.6688	2.96	16	−0.46
H(C)	0.1520	2.70	2	0.12
N	0.5852	3.25	14	−0.70
H(N)	0.000	0.00	2	0.415
C(Me)	0.5016	3.63	12	0.285
H(Me)	0.000	0.00	2	0.000

With this alloy composition for the container there would be no coherent neutron scattering contribution to the measured signal of the cell. During measurement the cell was maintained at ambient temperature ~25 °C. The scattering data were analyzed using neutrons wavelengths in the range $\lambda = 0.075-3.5$ Å over a corresponding Q-range for each data set of 0.1−30 Å^{-1}. After collection, the data were analyzed using the program Gudrun, available at ISIS.[39] These routines correct the data for the contributions from the empty cell, instrument background, absorption, and multiple scattering and normalize the data to absolute units using the scattering of a vanadium standard. The remaining corrections to account for the contributions from inelastic scattering by the sample, which for protons can have a pronounced dependence on the scattering vector, Q, was made using the method outlined previously.[40]

IV. EPSR Modeling

The technique of empirical potential structure refinement (EPSR)[31,32] has been used to build a three-dimensional model of the structure of liquid NMF that is consistent with the three measured total structure factors measured for C_2H_5ON, C_2D_5ON, and the 50% mixture. The first action in attempting to analyze the data using EPSR is to take a suitable reference potential energy function that will be used as the starting point for the subsequent structure refinement. The NMF model used has been previously optimized by one of us.[25] The reference potential between atom pairs was built from a combination of Lennard-Jones and Coulomb potential. Thus, the potential between atoms α and β would be represented by

$$U_{\alpha\beta}(r) = 4\varepsilon_{\alpha\beta}\left[\left(\frac{\sigma_{\alpha\beta}}{r}\right)^{12} - \left(\frac{\sigma_{\alpha\beta}}{r}\right)^{6}\right] + \frac{1}{4\pi\varepsilon_0}\frac{q_\alpha q_\beta}{r} \qquad (5)$$

where $\varepsilon_{\alpha\beta} = (\varepsilon_\alpha\varepsilon_\beta)^{1/2}$ and $\sigma_{\alpha\beta} = 0.5(\sigma_\alpha + \sigma_\beta)$ (the classical Lorentz−Berthelot mixing rules for the cross terms) and ε_0 is the permittivity of free space. The Lennard-Jones parameters, atomic masses, and fractional charges used to seed the modeling process are summarized in Table 1, and Table 2 summarizes the interactomic distances constraints used to define the basic molecular geometry of the molecule. In the simulations the liquid was constituted exclusively for the trans conformer, because about 95% of the molecules in the real liquid are from this conformer, as it has been discussed in the introduction.

The Monte Carlo simulation itself follows the traditional pattern,[41,42] with application of periodic boundary conditions, use of minimum image convention, and neighbor lists. The Lennard-Jones potential energy functions are truncated smoothly using a function of the form

$$T(r) = \begin{cases} 1 & r \le r_1 \\ 0.5\left[1 + \cos\pi\left(\dfrac{r - r_1}{r_2 - r_1}\right)\right] & r_1 < r < r_2 \\ 0 & r \ge r_2 \end{cases} \qquad (6)$$

where $r_1 = 9$ Å and $r_2 = 12$ Å, whereas the Coulomb potentials are truncated using the function

$$T_c(r) = \left(1 - \frac{r}{r_2}\right)^2\left(1 + \frac{8r}{5r_2} + \frac{2r^2}{5r_2^2}\right)\theta(r_2 - r) \qquad (7)$$

derived by Hummer et al.[43] within the reaction field approximation, with $\theta(r_2 - r)$ the Heaviside function.

The structure refinement was performed using an equilibrated cubic box of 500 NMF molecules with an atomic density of 0.091 68 Å^{-3}. An iterative procedure is used to drive the simulated structure toward agreement with the experimental data. This is achieved through the applications of perturbations to the intermolecular site−site potentials. These perturbations are derived iteratively from the difference between the measured diffraction data and the corresponding functions calculated from the evolving simulation.[32] It is interesting to stress then that the starting parameters are not altered during the simulations but the perturbation, which will constitute the empirical potential, is added to them during the simulations in such way a refinement in the structure is obtained. Once the structural model and associated perturbation potentials reach satisfactory agreement with the experimental data, the ensemble average structural information is accumulated. As the hydrogen bond to nitrogen within NMF is labile, there is an isotopic exchange of hydrogens between the nitrogens in the 50% mixture. This aspect has been taken into accounting in the isotopic weighting toward the intermolecular correlations.

V. Results and Discussion

Figure 2 shows the three independent experimental total structure factor and EPSR-refined model fits and residuals obtained for the three NMF samples. The overall quality of the fits is seen to be quite good although a little discrepancy between the empirical model and the experimental data is noticed at low frequencies to the fully protonated and the 50% mixture samples. Background and inelasticity corrections to the data are most difficult to do when the isotopomers contain light hydrogen and that may be in the origin of this misfit.

The total radial distribution functions, $f(r)$, that are obtained by direct Fourier transform of the inversion of the experimental structure factor data ($F(Q)$) and the corresponding functions calculated from the EPSR refined model are shown in Figure 3. Despite the ~1 Å discrepancy between the experimental data and the empirical potential for the protonated samples, the results indicate that the atomic bonds in the NMF model that contribute to the peaks in the range between about 1 and 2.5 Å are suitably represented. The slight imperfections in the molecular structure

TABLE 2: Intramolecular Geometric Parameters Used To Define the Basic Structure of NMF

atoms	C−H(C)	O−C	C−N	N−H(N)	N−C(Me)	C(Me)−H(Me)
distance (Å)	1.100	1.228	1.335	0.960	1.450	1.100
atoms	O−C−H(C)	O−C−N	C−N−H(N)	H(N)−N−C(Me)		
angle (deg)	120.5	122.9	119.8	118.3		
atoms	O−C−N−C(M)					
dihedral (deg)	0.0					

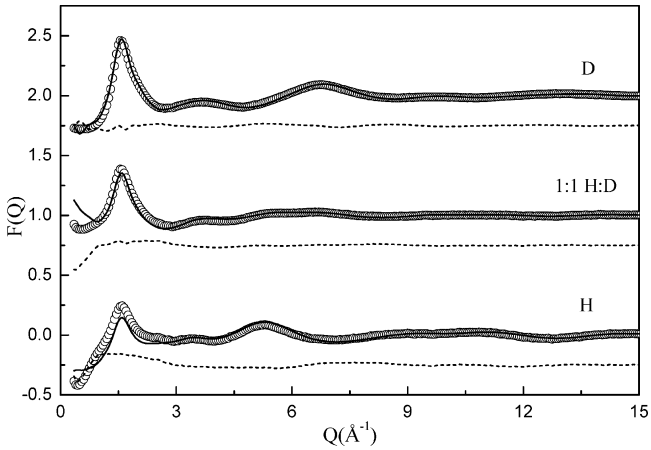

Figure 2. Experimentally measured total structure data (open circles) and EPSR refined fits (solid lines) for neutron scattering data collected on C_2NOH_5, a 50% mixture of C_2NOH_5 and C_2NOD_5, and C_2NOD_5. The fit residuals (broken lines) for each sample are shown vertically offset around −0.25, +0.75, and +1.75.

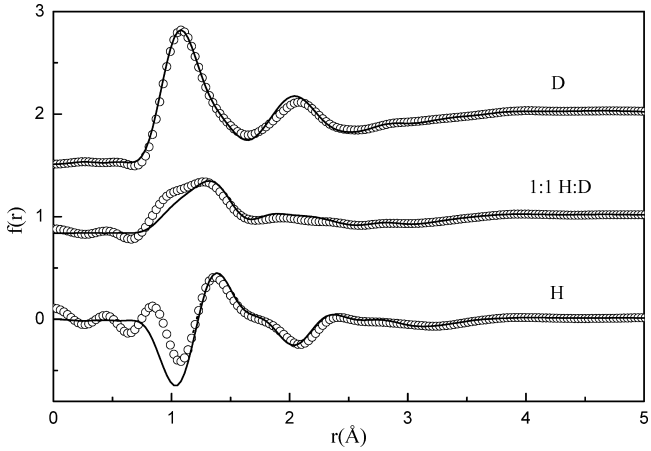

Figure 3. Composite radial distribution functions determined by direct Fourier transform of the experimental data (open circles) and EPSR refinement (solid lines) for neutron scattering data collected on C_2NOH_5, a 50% mixture of C_2NOH_5 and C_2NOD_5, and C_2NOD_5.

responsible for the discrepancies will not impact the intermolecular interactions significantly, as it has been discussed previously.[44]

The results shown in Figures 2 and 3 indicate the structure of the liquid is adequately represented by the empirical potential. Taking these results into account, the next natural step is to obtain the intermolecular site−site radial distribution functions ($g(r)$) for the liquid NMF. Some of the most important correlations are shown in Figures 4 and 5. Most of the $g(r)$ curves present narrow well-defined peaks instead of broad bands, which is a characteristic of well-structured liquids. In particular, the narrow O−H(N) peak with amplitude about 1.8 Å, is characteristic of H-bonding between the oxygen of one NMF molecule and the hydrogen bonded to nitrogen of a neighbor molecule.[4] It is interesting to draw attention to the fact that even correlations that are strongly repulsive due to the atoms having a charge of same sign, like O−N and C−C for instance, show narrow $g(r)$ peaks, which indicates that the hydrogen bond between the molecules is strong enough to keep them attached to each other, giving rise to a rather rigid multimolecular structure.

To give an idea on how the potential refinement has influenced the liquid $g(r)$ comparing with liquid simulations alone, Figure 6 compares some site−site correlations obtained

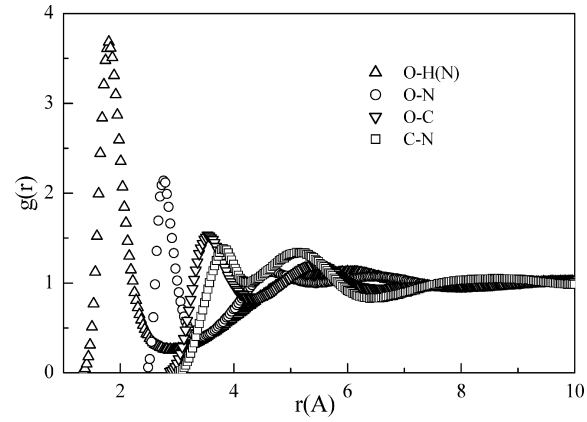

Figure 4. Site−site radial distribution functions derived by the EPSR calculations for the atom pairs displayed in the figure. (H)N is the hydrogen bonded to nitrogen in NMF.

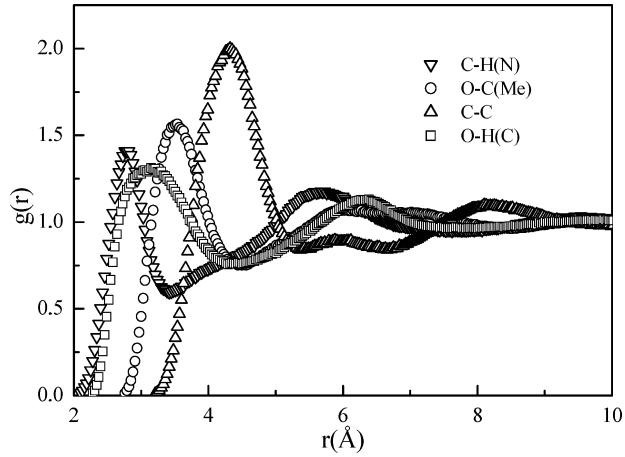

Figure 5. Site−site radial distribution functions derived by the EPSR calculations for the atom pairs displayed in the figure. (H)C is the hydrogen bonded to carbon, and C(Me) is the methyl carbon in NMF.

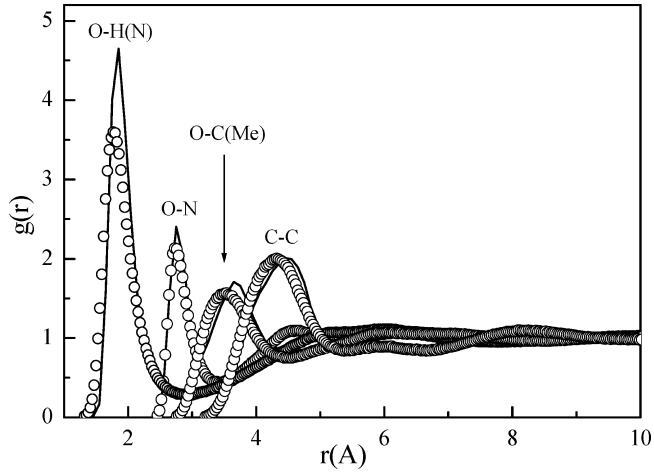

Figure 6. Some site−site radial distribution functions derived by the EPSR calculations (circles) and by Monte Carlo simulations without empirical potential refinement (line). (H)N is the hydrogen bonded to nitrogen in NMF, and C(Me) is the methyl carbon in NMF.

previously using Monte Carlo simulations[25] with the same correlations obtained in the present work. Two aspects must be stressed: the average distances between the molecules seem to be a little shorter in the present calculations, as well as the amplitude of the peak correlations, especially for the hydrogen bond peak. Taking into account the differences observed on each

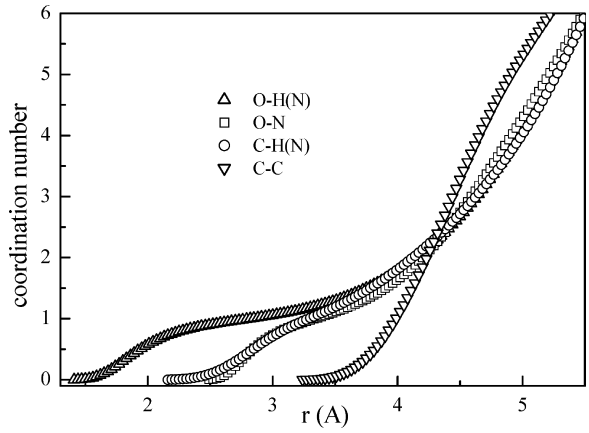

Figure 7. Coordination number as a function of distance for some representative site−site correlations in NMF. (H)N is the hydrogen bonded to nitrogen in NMF.

site−site correlations, it is apparent that the interactions between the molecules are a little stronger in the liquid (because of the $g(r)$ peaks are at shorter distances) than it is represented by the reference potential on its own. To explain the decrease in the peaks amplitude, however, is not so direct[45−47] and a deeper analysis is necessary to understand this difference. It is interesting to note that in the Monte Carlo simulations alone the molecules were kept rigid in the original geometry (parameters showed in Table 1), whereas in the present EPSR calculations the molecules are not strictly rigid: in addition to the Lennard-Jones potential for the intermolecular interactions, the atoms within the molecule were assumed to interact via harmonic potential with the force constants held sufficiently strong that the fluctuations mimic the observed zero point vibrational widths in the liquid. So, the molecules in the EPSR simulation have a chance to relax that they had not in the previous Monte Carlo simulations alone. Because of that, some differences in the interatomic correlations obtained from each type of calculation should be expected. Taking this aspect into account and that in the EPSR calculations, we have the experimental structure of the liquid obtained via the neutron diffraction analysis, whereas in the optimization of the reference molecular parameters just the heat of vaporization and the liquid density were used to fit the potential, one could expect that the present site−site correlation functions should be closer to the real ones than those obtained with the Monte Carlo simulations alone.

Plots of the coordination number as a function of the distance for some of the correlations are shown in the Figure 7. Most of the curves show well-defined flat plateaus, characteristics of well-structured coordination shells. Of course, this is a direct implication of the atomic site−site correlations pictured in the Figures 4 and 5. The curve for the C−C correlation, that is, in good approximation, the correlation of the center of mass of the molecule,[17] shows the shape characteristic of an uncharged spheres distribution.

Calculations of the coordination number for some of the most characteristics atom−atom correlations are listed in Table 3. The coordination number for the O−H(N) correlation, which has been attributed above to an intermolecular H-bond, is equal 1. The O−N coordination number is also equal to 1 with a minimum at 3.4 Å. These results indicate that such correlations are taking place between the same two molecules. As each NMF molecule can act as H-bond donor and acceptor, this pattern is a strong indication of formation of chains in the liquid structure, which is supported by the C−N coordination number. As the

TABLE 3: Coordination Numbers Obtained by Integration of the Curves from Zero up to a Point of Minimum in the Radial Distribution Functions Indicated[a]

correlation	r_{int}(Å)	r_{int} (Å)	coordination no. (atoms)
O−H(N)	2.85		1.00
O−N	3.4		1.05
C−N	4.2		1.9
C−N		6.4	10.7
O−C(Me)	4.5		3.05
C−C	5.3		5.7
C−C		6.7	11.9

[a] The C−C and C−N correlations have two points of minimum in the $g(r)$ plots (Figures 4 and 5).

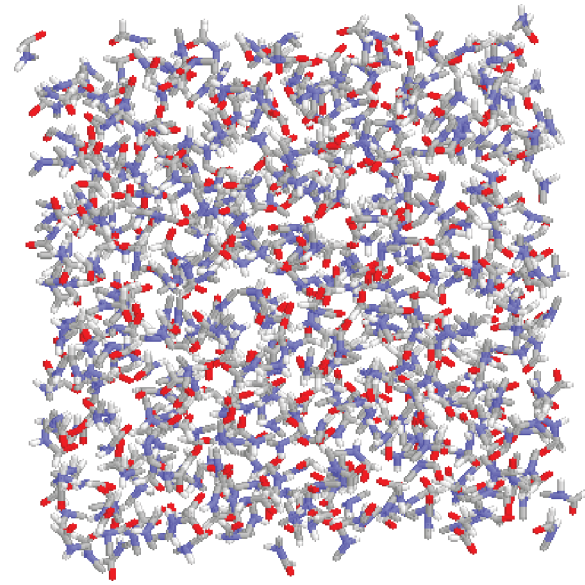

Figure 8. EPSR refined three-dimensional structure of liquid NMF.

carbon atom is, in a good approximation, at the center of the molecule, a C−N coordination number of about 2.0 with molecules up to a distance about 4.2 Å is the result of the coordination of the carbon atom of a NMF molecule with the nitrogen atom of the two neighbor molecules hydrogen-bonded to the central NMF. As evidence that the carbon atom is a good approximation for the center of the molecule, the C−C coordination number up to the distance of 6.7 Å is about 12, the number of closest neighbors for a close packing of neutral spheres. Curiously, there is a first minimum for that correlation around 5.3 Å, in which the coordination number is about half of the major coordination number, what indicates that, unlikely to a strictly distribution of uncharged particles, the solvation shell is somehow structured.

With the aim of identifying which liquid bulk patterns are in accord with these results, the file of the atom coordinates after the EPSR calculations was scanned with the program RASMOL,[48] trying to obtain a better insight of liquid structure. Figure 8 shows a "picture" of the "sample" where are easily identified cavities or canals through the bulk. These void regions are consequence of the oriented correlation between the molecules. Figure 9 shows the molecules within a sphere of radius 5 Å with the O−H(N) distances between some molecules written down in the caption. It is noted that there is a hydrogen-bonded trimer in this sphere (the molecules containing the atoms 1, 2, 3, and 4) with the O−H distances agreeing with the distances of the O−H correlation in the plots of Figure 4. Besides that, the molecules containing the atoms 9 and 10 would constitute a hydrogen-bonded dimer. Of course, if in a so tiny

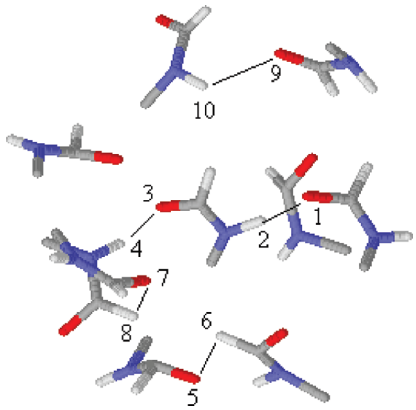

Figure 9. Molecules within a sphere of radius 5 Å captured from the liquid bulk. Distances between the atoms marked in the picture: 1−2, 1.56 Å; 3−4, 1.70 Å; 5−6, 2.75 Å; 7−8, 3.12 Å; 9−10, 2.44.

randomly chosen sphere one can easily finding such patterns, it is reasonable to suppose that the liquid bulk must be full up of them and even longer chains.

Nothing was discussed up to now about the characteristics of the O−H(C) correlation brought to light from this work and what could to be said concerning the so-called weak hydrogen bond in NMF based in the present results. As may be noticed by analyzing the $g(r)$ O−H(C) plot of Figure 5, the results show a well-defined peak for the O−H(C) correlation with maximum around 3 Å, which could be attributed to a weak hydrogen bond, taking into account what has been reported on that correlation.[5,49] This kind of hydrogen bond can play an important role in the stabilization of lots of structures,[5] and that may be the case in liquid NMF. The correlation is shorter than the O−C one, which indicates that the O−H(C) interaction orientates the relative intermolecular correlation. It is important to notice that in the cluster of molecules captured in Figure 9, there are two dimers, molecules containing the atoms 5, 6, 7, and 8, that would take part in the set of molecules that give rise to the O−H(C) correlation. Equally it could be claimed that the marked O−H(C) interaction is simply a consequence of packing effects which arise from the strong O−H(N) hydrogen bond. Molecular Mechanics and ab initio calculations on a cluster of molecules like the one shown here, could help having a better insight on the local NMF structure. This kind of calculation is being planned for the near future. Either way our results suggest that NMF is a highly structured liquid. This was an initial study of this material and future papers will describe solutions with nmf as solute and solvent as well.

V. Conclusions

The structure of NMF was investigated using neutron scattering with hydrogen−deuterium substitution and epsr simulations. Schoester et al.[17] and Neuefeind et al.[12,13] have used such isotope substitution in neutron diffraction to study the structure of NMF as well as other amides, but the level of detailing that the authors have achieved on the structure of NMF was not so rich as in the present case. Hammami et al. has investigated the structure of fully deuterated NMF,[16] but in a context rather different from ours. The use of EPSR simulation is believed to improve the quality of the intermolecular structural information that can be extracted from the raw diffraction data.[32,33,40] The present results suggest that the molecular model optimized by one of us previously[25] and that was used as the reference model in the present work mimics the liquid structure in a good way, but changes in the rdf are introduced by the potential refinement that can be understood as a improvement in the radial distribution functions. Of course, the availability of the experimental total structure factor used to fit the reference potential plays a major role in this improvement. The molecular relaxation used in the present simulations, against the rigid molecules used in the previous Monte Carlos simulations, however, may also be responsible for a fraction of the differences in the radial distribution functions. The site−site correlations obtained in the present simulations indicate a well-structured liquid with strong attractive interatomic interactions. Most of the $g(r)$ first neighbor peaks are narrow and well-defined. The results indicate that the liquid structure is driven by strong hydrogen-bonds between oxygen and the hydrogen bonded to nitrogen. These results agree with others, theoretical as well as experimental, published previously.[20−22,25] Taking into account the coordination number of the C−N correlation it is clear that any molecule is on average bonded to two others, which agrees with the fact that the molecules can act as hydrogen bond donor and acceptor. This strongly suggests the formation of molecular chains in the liquid as it has been reported previously by Ohtaki et al.[11] using X-ray diffraction. Our results showed the existence of dimers and trimers constituted for hydrogen-bonded molecules in little clusters of up to 5 Å radius, but of course, species bigger than those might exist in the liquid bulk. These results agree with the previous results published by Hammami et al.[15,16] The analysis of the O−H(C) correlation indicates that the weak hydrogen bond may play a important role in the stabilization of liquid NMF. If so, this interaction could be responsible for a sort of molecular framework in liquid NMF, which would contribute to its unusual dielectric and thermodynamic properties. It is interesting to note that, as the molecules are substantially slowed down by the strong hydrogen bonds between them, this favors the formation of weak hydrogen bonds which might not be seen in more mobile fluids. Moreover the hydrogen bonds have in general a cooperative character, so that once formed they have a stronger influence on the liquid properties than they would do if the same number of hydrogen bonds interacted independently of each other.

Acknowledgment. J.M.M.C. thanks the FAPESP (Fundação de Amparo à Pesquisa do Estado de São Paulo - Brazil) for supporting a stay at RAL-ISIS (process n. 2007/07513-2) and the ISIS Facility also for partial support for this visit.

References and Notes

(1) Oliveira, O. V.; Freitas, L. C. G. *J. Mol. Struct. (THEOCHEM)* **2005**, *728*, 179.
(2) Skarmoutsos, I.; Samios, J. *Chem. Phys. Lett.* **2004**, *384*, 108.
(3) Cordeiro, J. M. M. *Phys. Chem. Liq.* **2007**, *45*, 31.
(4) Jeffrey, G. A. *An Introduction to Hydrogen Bonding*; Oxford University Press: New York, 1997.
(5) Desiraju, G. R.; Steiner, T. *The Weak Hydrogen Bond*; Oxford University Press: Oxford, U.K., 1999.
(6) Garcia, B.; Alcalde, R.; Aparicio, S.; Leal, J. M.; Matos, J. S. *Phys. Chem. Chem. Phys.* **2001**, *3*, 2866.
(7) Riddick, J. A.; Bunger, W. B. *Techniques of Chemistry II* Wiley-Interscience: New York, 1970.
(8) Fantoni, A. C.; Caminati, W. *J. Chem. Soc., Faraday Trans.* **1996**, *92*, 343.
(9) Lide, D. R., Ed. *Handbook of Chemistry and Physics*, 83rd ed.; Wiley: New York, 2002.
(10) Kitano, M.; Kuchitsu, K. *Bull. Chem. Soc. Jpn.* **1974**, *47*, 631.
(11) Otaki, H.; Itoh, S.; Rode, M. *Bull. Chem. Soc. Jpn.* **1986**, *59*, 271.
(12) Neuefeind, J.; Chieux, P.; Zeidler, M. D. *Mol. Phys.* **1992**, *76*, 143.
(13) Neuefeind, J.; Zeidler, M. D.; Poulsen, H. F. *Mol. Phys.* **1996**, *87*, 189.
(14) Hammami, F.; Nasr, S.; Oumezzime, M.; Cortes, R. *Biomol. Eng.* **2002**, *19*, 201.

(15) Hammami, F.; Bahri, M.; Nasr, S.; Jaidane, N.; Oumezzime, M.; Cortes, R. *J. Chem. Phys.* **2003**, *119*, 4419.
(16) Hammami, F.; Nasr, S.; Bellisent-Funel, M. C. *J. Chem. Phys.* **2005**, *122*, 1.
(17) Schoester, P. C.; Zeidler, M. D.; Radnai, T.; Bopp, P. A. *Z. Naturforsch A* **1995**, *50*, 38.
(18) Gao, J.; Pavelites, J. J.; Habibollazadeh, D. *J. Phys. Chem. A* **1996**, *100*, 2689.
(19) Hirst, J. D.; Hirst, D. M.; Brooks, C. L. *J. Phys. Chem. A* **1997**, *101*, 4821.
(20) Desfrancois, C.; Periquet, V.; Carles, S.; Schermann, J. P.; Smith, D. M. A.; Adamowicz, L. *J. Chem. Phys.* **1999**, *110*, 4309.
(21) Torii, H.; Tasumi, M. *J. Phys. Chem A* **2000**, *104*, 4174.
(22) Headley, A. D.; Nam, J. *J. Mol. Struct (THEOCHEM)* **2002**, *589*, 423.
(23) Nandini, G.; Sathyanarayana, D. N. *J. Mol. Struct (THEOCHEM)* **2002**, *579*, 1.
(24) Martinez, A. G.; Vilar, E. T.; Fraile, A. G.; Martinez-Ruiz, P. *J. Phys. Chem. A* **2002**, *106*, 4942.
(25) Cordeiro, J. M. M. *Int. J. Quantum Chem.* **1997**, *65*, 709.
(26) Fantoni, A. C.; Caminati, W.; Hartwig, H.; Stahl, W. *J. Mol. Struct.* **2002**, *612*, 305.
(27) Cordeiro, J. M. M.; Cordeiro, M. A. M.; Bosso, A. R. S. A.; Politi, J. R. S. *Chem. Phys. Lett.* **2006**, *423*, 67.
(28) Barthel, J.; Buchner, R.; Wurm, B. *J. Mol. Liq.* **2002**, *98*, 329.
(29) Finney, J. L.; Soper, A. K. *Chem. Soc. Rev.* **1994**, *23*, 1.
(30) McGreevy, R. L. *J. Phys.: Condens. Matter* **2001**, *13*, R887.
(31) Soper, A. K. *Chem. Phys.* **1996**, *202*, 298.
(32) Soper, A. K. *Phys. Rev. B* **2005**, *72*, 104204.
(33) Bowron, D. T.; Finney, J. L.; Soper, A. K. *J. Am. Chem. Soc.* **2006**, *128*, 5119.
(34) Soper, A. K. *Mol. Phys.* **2001**, *99*, 1503.
(35) Soper, A. K. *Chem. Phys.* **2000**, *258*, 121.
(36) Bowron, D. T.; Finney, J. L.; Soper, A. K. *J. Phys. Chem. B* **1998**, *102*, 3551.
(37) Hardacre, C.; Holbrey, J. D.; McMath, S. E. J.; Bowron, D. T.; Soper, A. K. *J. Chem. Phys.* **2003**, *118*, 273.
(38) Thompson, H.; Wasse, J. C.; Skiper, N. T.; Howard, C. A.; Bowron, D.; Soper, A. K. *J. Phys.: Condens. Matter* **2004**, *16*, 5639.
(39) Soper, A. K.; Howells, W. S.; Hannon, A. C. Report No. RAL-89-046, 1989.
(40) Soper, A. K.; Luzar, A. *J. Chem. Phys.* **1992**, *97*, 1320.
(41) Allen, M. P.; Tildesley, D. J. *Computer Simulation of Liquids*; Oxford University Press: Oxford, U.K., 1987.
(42) Frenkel, D.; Smith, B. *Understanding Molecular Simulation: from Algoritms to Applications*; Academic Press: New York, 1996.
(43) Hummer, G.; Soumpasis, D. M.; Newmann, M. *J. Phys.:Condens. Matter* **1994**, *6*, A141.
(44) Chandrasekhar, J.; Jorgensen, W. L. *J. Chem. Phys.* **1982**, *77*, 5073.
(45) Soper, A. K.; Weckstrom, K. *Biophys. Chem.* **2006**, *124*, 180.
(46) Soper, A. K.; Finney, J. L. *Phys. Rev. Lett.* **1993**, *71*, 4346.
(47) Turner, J.; Soper, A. K.; Finney, J. L. *Mol. Phys.* **1992**, *77*, 411.
(48) Sayle, V. *Molecular Visualization Program, RasMol V2.5*; Glaxo Research and Development: Greenford, Middlesex, U.K., 1999.
(49) Cordeiro, J. M. M. *J. Braz. Chem. Soc.* **2004**, *15*, 351.

JP902053Y